Path Planning for Shop-Floor Material Transfer Robots Incorporating Particle Swarm and Ant Colony Algorithms

Yan HAN*, Tao SONG

School of Intelligence Technology, Geely University, No. 123, SEC. 2, Chengjian Avenue, Eastern New District, Chengdu City, Sichuan Province, 610000, China
hanyan@guc.edu.cn (**Corresponding author*), songtao@guc.edu.cn

Abstract: To enhance the path planning capability of material transfer robots during shop-floor operations, an improved path planning method with particle swarm and ant colony algorithms based on the characteristics of materials is proposed. First, the improved particle swarm grouping method containing elite subpopulations is proposed to increase the population diversity and solve the following problem: the algorithm is easy to fall into the local optimum. Moreover, the parameters are adaptively adjusted to enhance the particle search ability. Second, a bidirectional search strategy is utilized to enhance ant utilization and optimize the algorithm's speed. Finally, a marking grid is set to enhance the safety of the robot operation, and the path is smoothed using cubic B-spline curves, thereby reducing the robot's energy consumption. The simulation results reveal that the algorithm can effectively enhance path-planning efficiency and provide a basis for further research on the application of robot path-planning algorithms for material transfer in shop-floor environments.

Keywords: Material transfer robots, Characteristics of materials, Particle swarm grouping, Elite subpopulations.

1. Introduction

Currently, the in-factory material transfer work tends to intelligent development in the manufacturing industry's traditional factory, thus transforming one of the crucial smart-factory components (Saber, Behiry & Amin, 2022). Material transfer robots are a novel category of industrial machinery and equipment and exhibit the following advantages: they enhance the efficiency of material handling operations and can somewhat realize the advantages of cost reduction and efficiency in the manufacturing industry (Chai & Xia, 2023). In the shop-floor environment, robots work in a wide variety of environments, and, simultaneously, there are requirements for robot efficiency (Šegota* et al., 2022). It is, therefore, necessary to select the appropriate industrial robot according to the type of work in the shop-floor (Ibrahim et al., 2022). For example, the material transfer robots analysed herein are mobile. In the automotive industry, it is necessary to consider the handling of materials in the final assembly, stamping, welding, and painting shop floors. How to make material transfer robots safely avoid obstacles while improving the material transfer efficiency is an urgent problem (Mani et al., 2023).

Moreover, the shop-floor environment encompasses a variety of materials, including standardized, non-standardized, and externally processed materials. When employing traditional path planning methods for transporting these diverse materials, transport robots face challenges such as extended transportation routes, heightened energy consumption, and potential collisions with obstacles (Wang et al., 2022a). Hence, this paper's primary objective is to enhance the efficiency of shop-floor transfer robots during material transportation within the shop-floor setting.

The structure of the paper is as follows: Section 2 presents a review of the relevant literature, Section 3 describes the research methodology for path planning, Section 4 discusses the simulation experiments, and Section 5 presents the conclusions.

2. Literature Review

Currently genetic algorithms (GA) (Wen et al., 2021), A* algorithms (Zhong et al., 2020) and ant colony optimization (ACO) (Gu et al., 2020) are often utilized to solve transfer robots path planning problems. When solving the robot path planning problem, the advantages of the algorithms are rationally analysed, and the combination of multiple algorithms can be utilized collaboratively to achieve ideal results (Haider et al., 2022).

One study addressed the problem of path planning methods for handling robots being prone to local optima and lacking universal adaptability to the environment. The authors incorporated the species evolution concept of genetic algorithms and redefined simulated annealing coefficients and grid coefficients. The improved algorithm shortens the length of path planning of handling robots (Tao et al., 2018). Researchers aimed to enhance the efficiency and stability of automated guided vehicle (AGV) material transportation within workshops, by employing a fusion algorithm that

https://doi.org/10.24846/v33i3y202405

combines genetic and particle swarm algorithms for path planning. They utilized the Warshall-Floyd algorithm to determine optimal paths between any two points and proposed a particle iteration mechanism based on time priority to expedite algorithm convergence (Du et al., 2019). To address the suboptimal path optimization efficiency of sorting and handling robots, they integrated the A* algorithm with the ant colony algorithm. They utilized the A* algorithm to identify an optimal route distribution pheromone and, based on varying parameters, selected path nodes for planning to minimize material transportation duration (Cai et al., 2018).

A research subject emphasized the shortest material transportation path for automatic guided vehicles, reducing redundant nodes and corners through secondary path planning on the initial path outlined by the A* algorithm (Zhang et al., 2019).

One study applied the simulated annealing method to address the local minimum issue encountered with the artificial potential field algorithm, consequently reducing the operational path of transport robots (Zhu et al., 2020).

Certain studies employed an enhanced particle swarm optimization algorithm to devise the shortest path for enhancing the material transportation efficiency of robots. Cross operation was utilized to update particle positions, while a mutation mechanism was integrated to prevent the algorithm from converging to local optima (Tao et al., 2021). To reduce the length of the robot's driving path in the shop-floor, they employed Tent chaotic mapping to refine Wolf initialization. They further refined the Wolf evolution method based on genetic principles, enhancing the algorithm's convergence capability (Zhou, 2020).

Other research studies allocated transportation task sequences between shelves and processing equipment to corresponding AGVs, formulated the initial path for each AGV, and devised collision-free global routes for multiple AGVs within the workshop, aiming to minimize overall transportation time (Wang et al., 2022b).

Some other studies addressed the following problem: the efficiency of the A* algorithm can be significantly degraded in a large logistics factory environment. The length of the movement path and the number of turns are reduced by changing the total cost formula, and the five-point cubic smoothing method is introduced to increase the smoothness of the movement path. Thus, the handling robot's energy consumption is reduced (Zhang & Wu, 2023). Researchers focused on enhancing the transportation efficiency of carrying robots in loom workshops. They employed Bessel curve smoothing paths to optimize robot transportation efficiency and improved the algorithm's heuristic function, through a multi-segment dynamic weighting method, to expedite path search. Through simulated large loom workshop environments, the refined algorithm accelerated path planning (Gong et al., 2023).

A recent study integrated diagonal distance and turning weight into the heuristic function of the A* algorithm to address excessive corners and extended transportation times encountered by workshop guided vehicles (Liu et al., 2024).

A research subject addressed the optimization of path selection and safe operation for cleaning robots in wood processing workshops, by employing multiple sensors in conjunction with a genetic algorithm for path planning (Zhou et al., 2014). Aiming at improving the safety and efficiency of warehouse robot path planning, they integrated the influence of unknown factors, simulated by a Poisson distribution, to refine and smoothen the path charted by the ant colony algorithm, thereby crafting an optimal route (Chen et al., 2023).

The aforementioned approaches address various challenges in the path planning of transportation robots for material conveyance, such as shortening path lengths, reducing energy consumption through path smoothing, and ensuring collision-free operation for enhanced safety. However, these methods do not tailor path planning schemes to the specific characteristics of the transported materials. In a static environment, a uniform route planning approach fails to differentiate the size and weight of materials transported on each occasion. Implementing a sub-strategy transportation method could bolster efficiency.

3. Research Methodology

This paper supports the idea that transfer robots employ distinct static path planning methods tailored to the characteristics of shop-floor materials, thereby enhancing transportation efficiency. For standard materials, as depicted in Figure 1(a), an improved particle swarm algorithm and the ant colony algorithm are proposed for robot path planning. To address the shortcomings of traditional

algorithms, population diversity was increased, using clustering of elite particles. To optimize algorithm convergence, the study improved learning factors and dynamically adjusted inertia weights. The bidirectional search strategy is applied to enhance ant utilization and optimize algorithm speed. Meanwhile, the solution of the particle swarm algorithm is utilized as the basis for adjusting the initial path pheromone of the ant colony algorithm, which is applied to solve the global optimal path. For longer size materials, as depicted in Figure 1(b), a marking grid is set to enhance the safety of the robot operation. For heavier materials, as depicted in Figure 1(c), this study utilized cubic B-splines to smooth the path and reduce the robot's energy consumption. Thus, this study provides a basis for further research on the application of robot path-planning algorithms to the problem of material transfer in a shop-floor environment.

(a) Standard (b) Longer size (c) Heavier

Figure 1. Diverse materials

3.1 Environmental Modelling

The application of this algorithm is verified in the shop-floor environment, and the grid method is used to establish a simulation map. Herein, the grid method is utilized to build the operating environment of the shop-floor material transfer robot, because the method is intuitive in expression and easy to store (Liu et al., 2023). When modelling the environment, the material transfer robot is considered as a mass (Hao, 2022). The shop-floor environment is mapped to a certain scale on the grid map. Static obstacles in the shop floor, such as pallets, sheet metal, and tooling are represented by a black grid. The unobstructed environment in the shop floor is represented by a white grid. The grid modelling method that is utilized to construct the shop-floor environment is illustrated in Figure 2.

To minimize the total path length, the objective function is formulated as:

$$f(x)=\sum_{i=1}^{n-1} d\left(x_i, x_{i+1}\right) \tag{1}$$

where $x=(x_1,x_2,\ldots,x_n)$ represents the sequence of nodes in the path, $d(x_i, x_{i+1})$ is the distance between the nodes x_i and x_{i+1}, and n is the number of nodes in the path.

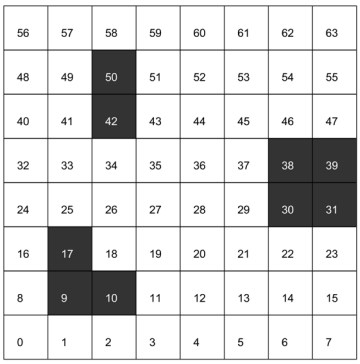

Figure 2. Environmental modeling

Because the shop materials are planned by the industrial engineering department staff, the shape and placement of the material footprint are more organized, as depicted in Figure 3.

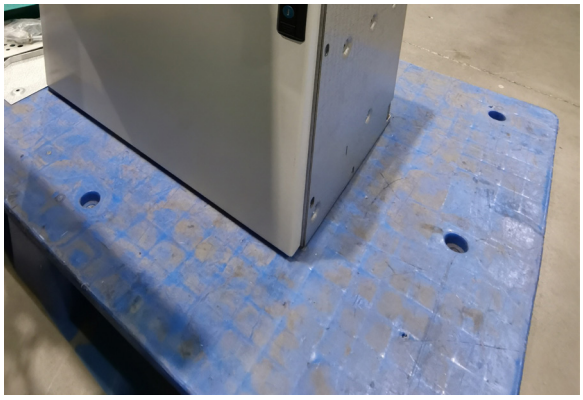

Figure 3. Static obstacles

3.2 Improved Particle Swarm Grouping

Particle swarm optimization (PSO) are bionic algorithms that simulate the foraging of a flock of birds (Chen et al., 2022). In particle swarm optimization, each particle represents a candidate solution. The optimal solution is obtained by constantly updating their information (Tao et al., 2023). In the N-dimensional environment, the particle population is m. The position of particle i is expressed as $x_i=\{x_{i1},x_{i2},\ldots,x_{iN}\}$. The particle iteratively updates the position x to search for the optimal position. The velocity of particle i is expressed as $v_i=\{v_{i1},v_{i2},\ldots,v_{iN}\}$. The equations for the change of velocity and position of particle i in the D-dimensional component ($1\leq d\leq N$) of the search space are as follows:

$$v_{id}(t+1)=\omega v_{id}(t)+c_1 r_1\left(p_{id}(t)-x_{id}(t)\right)+c_2 r_2\left(p_{gd}(t)-x_{id}(t)\right) \tag{2}$$

$$x_{id}(t+1)=v_{id}(t+1)+x_{id}(t) \tag{3}$$

where t denotes the number of iterations, $p_{id}(t)$ denotes the D-dimensional component of the particle searching for the optimal position at the t iteration, $p_{gd}(t)$ denotes the D-dimensional component of the global optimal position searched by the t iteration of the particle swarm, ω denotes the inertial weight, c_1 and c_2 denote the accelerators, and r_1 and r_2 denote random numbers between [0,1].

The particle swarm grouping algorithm yields more optimal results compared to the single-population particle swarming algorithm. This paper proposes an improved particle grouping method incorporating subgroups. The particles are sorted by their individual fitness values, in descending order, then are divided into M subgroups. The particles are specifically allocated from the sorted list to each subgroup, sequentially, starting from the first subgroup, until the Mth subgroup. After completing one cycle of allocation, the remaining particles from the first subgroup continue to be allocated again, until all particles are allocated. For each subgroup, the particle with the highest fitness value is identified as the best particle in that subgroup. Moreover, an elite subpopulation is established, and the optimal particles are placed into that population. The elite subgroup is responsible for global search optimization, and the remaining subgroups are responsible for local search optimization.

3.3 Dynamic Parameter Adjustment

The regular particle velocity and position formulas are first updated, and if the particle fitness values cannot be improved after use, the following formulas are utilized:

$$v^*_{id}(t+1) = \omega_r v_{id}(t) + c_{a1} r_1 \left(p_{id}(t) - x_{id}(t)\right) + c_{a2} r_2 \left(p_{gd}(t) - x_{id}(t)\right) \quad (4)$$

$$x_{id}^*(t+1) = v^*_{id}(t+1) + x_{id}(t) \quad (5)$$

Herein, a kind of acceleration factor c_{a1} *and* c_{a2}, which becomes nonlinear with the number of iterations and dynamic adjustment of inertia weight, is utilized to obtain ω_r.

$$c_{a1} = c_{1\max} + (c_{1\min} - c_{1\max})(\frac{n_1}{n_2})^2 \quad (6)$$

$$c_{a2} = c_{2\max} + (c_{2\min} - c_{2\max})(\frac{n_1 - n_2}{n_2})^2 \quad (7)$$

$$\omega_r = \omega_{\min} + (\omega_{\max} - \omega_{\min})\frac{d}{d\max} \quad (8)$$

where c_{1max}, c_{1min} denote the maximum and minimum values of c_1; c_{2max}, c_{2min} denote the maximum and minimum values of c_2; n_1 denotes the number of current iterations; and n_2 denotes the total number of iterations. Moreover, d denotes the Euclidean distance between the current particle and the optimal particle within the subpopulation, and dmax denotes the maximum distance between the current particle and the optimal particle of all subpopulations at the time of iteration. ω_{max} denotes the maximum weight coefficient, ω_{min} denotes the minimum weight coefficient. The parameters for the simulation experiments in this study are set as follows: ω_{max}=0.9, ω_{min}=0.4.

3.4 Bidirectional Search Strategy

Ant colony algorithms are derived from bionic evolutionary algorithms that simulate the behaviour of ant colonies (Wu et al., 2023). Each ant leaves a certain amount of pheromone concentration on the path it travels, and the algorithm can be optimized by changing the value of this concentration (Gao et al., 2020). The ants update the local pheromone concentration as they move from grid i to the next grid j. When the ant colony completes an iteration, the global pheromone concentration is updated (Pu et al., 2023). The transfer probability for the ants is as follows:

$$P_{ij}^k(t) = \begin{cases} \dfrac{\tau_{ij}^{\alpha}(t)\eta_{ij}^{\beta}(t)}{\sum_{s\in C}\tau_{is}^{\alpha}(t)\eta_{is}^{\beta}(t)} & j \in C \\ 0 & else \end{cases} \quad (9)$$

$$\eta_{ij} = \frac{1}{d_{ij}} \quad (10)$$

where $P_{ij}^{\ k}$ denotes the probability that the k^{th} ant moves from node i to node j; τ_{ij} denotes the pheromone level on the path from node i to node j; η_{ij} denotes the heuristic factor of the path from node i to node j; α denotes the pheromone factor; β denotes the expected heuristic factor; and C is the set of paths that the k^{th} ant is allowed to choose from at this stage. d_{ij} denotes the linear distance between the current node i and the next optional node j.

To more optimally utilize the search ability of individual ants, an iterative approach with foldback is proposed. However, this approach leads to interference of the forward pheromone with the reverse pheromone. Herein, an improved strategy is utilized. When an individual ant reaches the target point from the starting point, the pheromone is updated. After completing a path search, the

ant returns to the starting point and updates the pheromone levels to complete one iteration. This iterative process not only reduces the waiting time during searches, but also increases the efficiency of ant reuse, thereby improving the overall search efficiency. When choosing a path based on the transfer probability formula, the relationship with the goal point, the starting point, is not involved, since only the relationship between the current node and the neighbouring nodes is considered. Thus, the algorithm is prone to problems, such as inaccurate search or slow convergence when searching for paths.

Therefore, an improved heuristic function is introduced: the study introduces the current optional straight-line distance of the next node from the end point into the mix. Moreover, the straight-line distance of the current node from the start point is introduced, which leads to better guiding of the search direction, narrowing of the search area, and enhanced search efficiency. Different heuristic functions are utilized in the forward search and reverse re-entry processes.

The heuristic function from the starting point to the goal point can be expressed as:

$$\eta_e = \frac{1}{d_{ij} + d_{je}} \tag{11}$$

where d_{je} denotes the straight-line distance between the current node j and the target point e.

The heuristic function from the target point to the starting point can be expressed as:

$$\eta_s = \frac{1}{d_{ij} + d_{js}} \tag{12}$$

where d_{js} denotes the straight-line distance between the current node j and the start point s.

3.5 Fusion Algorithm

The fusion algorithm steps are as follows:

Step 1: Initialize the algorithm parameters;

Step 2: Calculate the fitness value of each particle, group the particles into clusters based on the fitness value, and place the optimal particles into the elite subclusters;

Step 3: Update the particles' individual and global optimal solutions;

Step 4: During the algorithm search process, the particle velocity and position are updated as per formulas (2) and (3). If the particle fitness value is not improved, the particle velocity and position are updated according to formulas (4) and (5). If the subgroup optimal solution is more optimal than the global optimal solution, the worst solution in the elite subgroup is replaced with the subgroup optimal solution;

Step 5: Determine whether the set maximum number of iterations has been attained. If so, the pheromone on the path of the ACO algorithm is adjusted with the obtained optimal solution; otherwise, return to Step 3;

Step 6: Adjust the pheromone on the path according to the optimal solution obtained by the improved particle swarm algorithm;

Step 7: Set M ants to conduct path searches, according to the bidirectional search strategy;

Step 8: When all ants have finished searching the target space, they are updated according to the global pheromone update formula;

Step 9: Output the optimal path at this point.

The flowchart of the fusion algorithm is depicted in Figure 4.

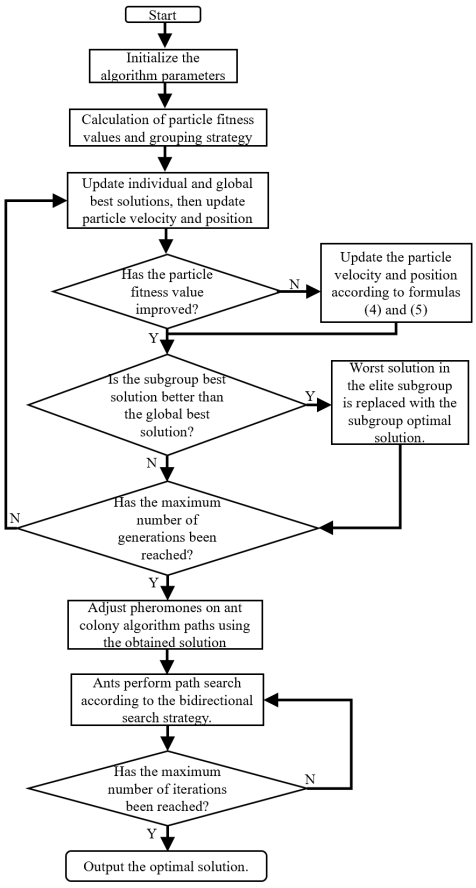

Figure 4. Flowchart of the fusion algorithm

According to the working environment of the robot, the fusion algorithm is further optimized. The robot can choose the optimal path, the safest path, and the path with the lowest energy consumption, according to the algorithm selection, based on the characteristics of the material to be transported.

3.6 Security-Marking Grid

This aspect needs to be taken into account, because the materials transported by shop-floor material transfer robots exhibit a specific mechanical dimensionality. For example, the size of some materials is long, and there is a scenario of brushing against obstacles when passing through them. Even if the path does not cross the boundary of an obstacle in the simulation environment, a certain safety distance should be ensured for materials with long dimensions. Therefore, a safe obstacle-avoidance strategy is utilized to ensure the safety of a shop-floor material transfer robot during shop-floor operations.

This strategy identifies the grids, and the algorithm solves the path to avoid the path contacting with the obstacle grids; thus, enhanced path security is achieved. A schematic diagram of the path coming into contact with the obstacle grid is illustrated in Figure 5(a). The path after the introduction of the marker grid is depicted in Figure 5(b). The path is further optimized by using the simplified operator. Figure 5(c) indicates the optimized path after the simplified operator processing.

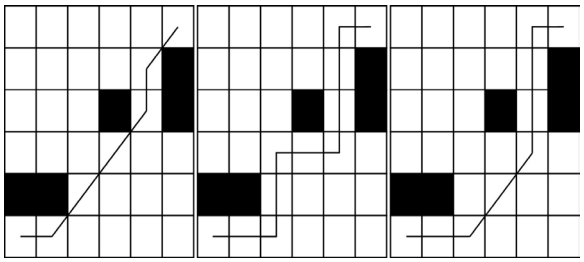

(a) Contact (b) Marking (c) Simplified

Figure 5. Result of security-marking grid

3.7 Cubic B-spline Smooth Path

Because the fusion algorithm produces path spikes when turning, the transshipment robot should smooth the path, if it needs to reduce the robot's wear and tear and energy consumption when transporting heavier materials (Gültekin, Diri & Becerikli, 2023). Herein, path spikes are smoothed using cubic B-spline curves. Smooth path steps are as follows:

Step 1: B-spline curve parameters are set;

Step 2: The optimal path nodes output is saved by the fusion algorithm;

Step 3: The optimal path nodes are utilized as control points to generate B-spline curves;

Step 4: The B-spline curve is output and the algorithm ends.

4. Results and Discussions

The simulation environment comprises two 20×20 grid maps. The obstacle coverage for Scene 1 is 33.24%. The obstacle coverage for Scene 2 is 51.80%. (1, 1) denotes the robot's starting point coordinates and (20, 20) denotes its end point coordinates. By varying the parameter values and observing the changes in algorithm performance, the optimal parameter combination can be determined. In this study, the sparrow search algorithm and genetic algorithm are initialized exclusively for the purpose of performance comparison with the fusion algorithm. The parameters of the particle swarm algorithm are as follows: number of particles $NP=50$, $\omega=0.5$, $c_{1max}=c_{2max}=2.5$, $c_{1min}=c_{2min}=0.5$. The parameters of the ant colony algorithm are as follows: number of ants $M=50$, $\alpha=1$, and $\beta=12$. The parameters of the genetic algorithm are as follows: number of individuals in the first-generation $N=50$, crossover probability $P_c=0.8$ and mutation probability $P_m=0.3$. The parameters of the sparrow search algorithm are as follows: number of sparrows $NP=50$, safety value = 0.8, discoverer ratio $RP=0.3$, and scout ratio $SP=0.2$. To rule out randomness in the algorithm's optimization results, all four algorithms were run independently for 30 times.

4.1 Shortest Path Results in Scene 1

The path planning results of sparrow search algorithm (SSA), GA, PSO, and PSO-ACO in Scene 1 are illustrated in Figures 6(a), 6(b), 6(c), and 6(d). The iterative convergence curves are depicted in Figure 7, while the experimental data are depicted in Table 1.

The shortest path length of PSO-ACO is 3.02%, 3.94%, and 8.29% shorter than the one of SSA, GA, and PSO, respectively; the average path length of PSO-ACO is 13.17%, 8.58%, and

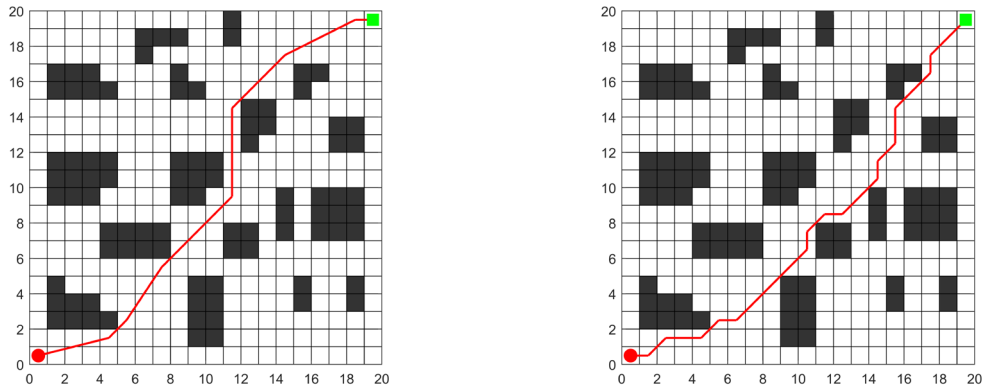

(a) SSA (b) GA

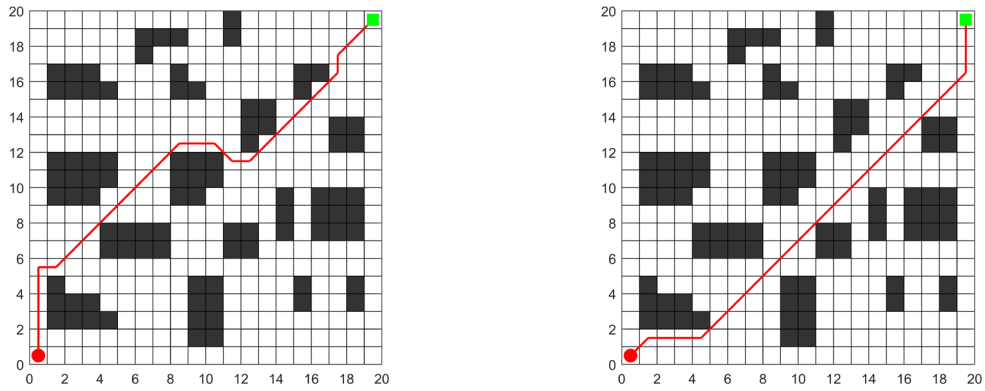

(c) PSO (d) PSO-ACO

Figure 6. The optimal path comparison of four algorithms in Scene 1

14.31% shorter than the one of SSA, GA, and PSO, respectively; the minimum number of corners of PSO-ACO is 50%, 80% and 62.5% lower than the one of SSA, GA, and PSO, respectively; the mean value of the number of corners of PSO-ACO is 57.14%, 81.25%, and 70% lower than the one of SSA, GA, and PSO, respectively; the minimum value of the number of iterations of PSO-ACO is 22.73% lower than the one of GA and 61.36% lower than the one of PSO; the mean value of the number of iterations is reduced by 40%, 27.78%, and 74.65% compared to the one of SSA, GA, and PSO, respectively.

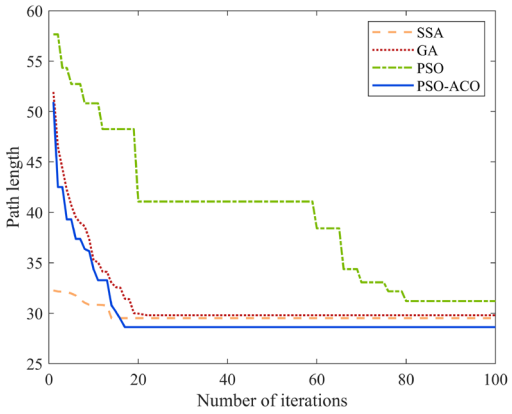

Figure 7. Iterative convergence curves in Scene 1

Table 1. Comparison of experimental data in Scene 1

Algorithm	Optimal path length		Number of turns		Iterations	
	Optimal value	Average value	Optimal value	Average value	Optimal value	Average value
SSA	29.5145	32.9661	6	7	14	30
GA	29.7990	31.3102	15	16	22	23
PSO	31.2100	33.4047	8	10	44	71
PSO-ACO	28.6240	28.6240	3	3	17	18

4.2 Shortest Path Results in Scene 2

The path planning results for SSA, GA, PSO, and PSO-ACO in Scene 2 are illustrated in Figures 8(a), 8(b), 8(c), and 8(d). The iterative convergence curves are illustrated in Figure 9, while the experimental data are illustrated in Table 2.

The shortest path length of PSO-ACO is 2.90%, 1.94%, and 5.57% shorter than the one of SSA,

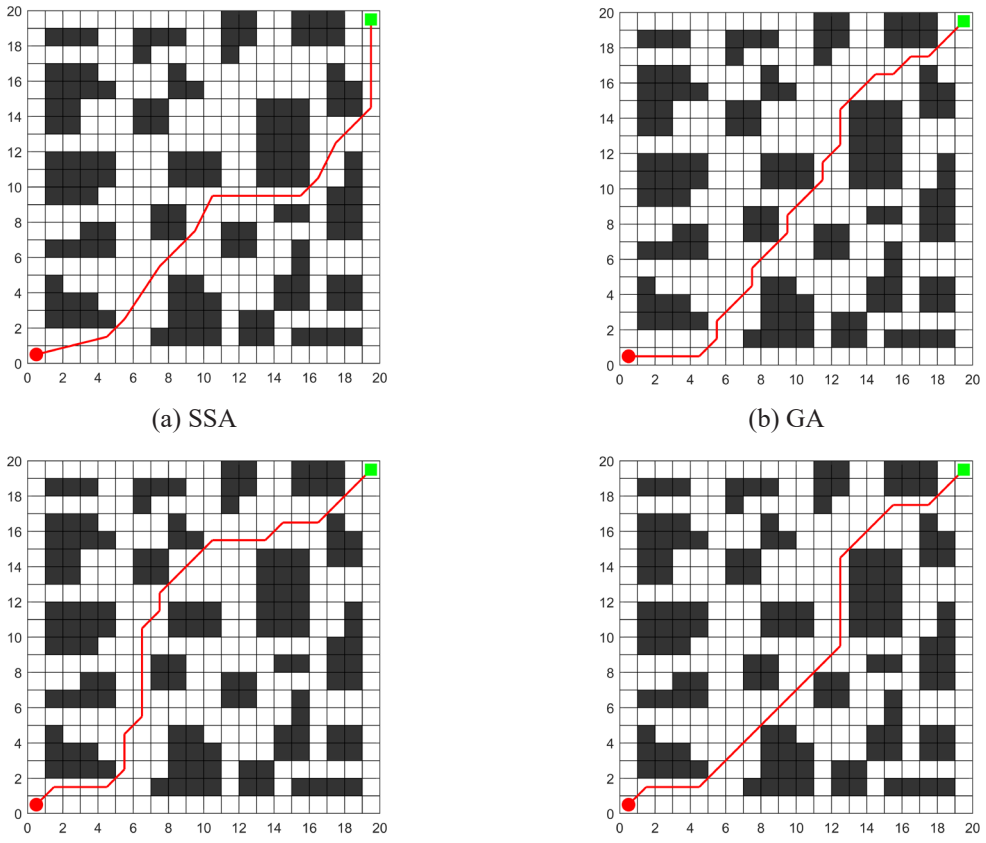

(a) SSA (b) GA

(c) PSO (d) PSO-ACO

Figure 8. The optimal path comparison of four algorithms in Scene 2

Table 2. Comparison of experimental data in Scene 2

Algorithm	Optimal path length		Number of turns		Iterations	
	Optimal value	Average value	Optimal value	Average value	Optimal value	Average value
SSA	30.6861	33.2445	7	8	16	27
GA	30.3848	32.7061	15	17	20	23
PSO	31.5540	33.3227	12	14	63	82
PSO-ACO	29.7960	29.7960	6	6	19	21

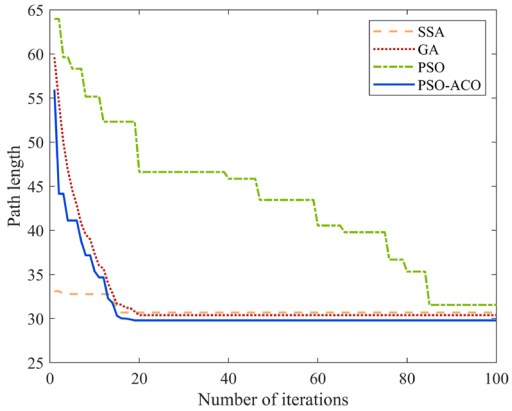

Figure 9. Iterative convergence curves in Scene 2

GA, and PSO, respectively; the average path length of PSO-ACO is 10.37%, 8.90%, and 10.58% shorter than the one of SSA, GA, and PSO, respectively; the minimum number of corners of PSO-ACO is 14.29%, 60% and 50% lower than the one of SSA, GA, and PSO, respectively; the mean value of the number of corners of PSO-ACO is 25%, 64.71%, and 57.14% lower than the one SSA, GA, and PSO, respectively; the minimum value of the number of iterations of PSO-ACO is 5% lower than the one of GA and 69.84% lower than the one of PSO; the mean value of the number of iterations of PSO-ACO was reduced by 22.22%, 8.70%, and 74.39% compared to the one of SSA, GA, and PSO, respectively.

4.3 Path Planning Results that Contain Security Identifiers

The fusion algorithm, that incorporates the security marking grid in Scene 1 and Scene 2, respectively, is run. Figures 10 and 11 indicate that no contact with the obstacle grids occurred on the robot travel path. The optimal path lengths are 29.2132 and 32.1421, respectively. The number of corners is 7 and 13, respectively. This optimization method focuses on the safety of the path, which increases the path length, but also ensures the safety of the transport robot during operation.

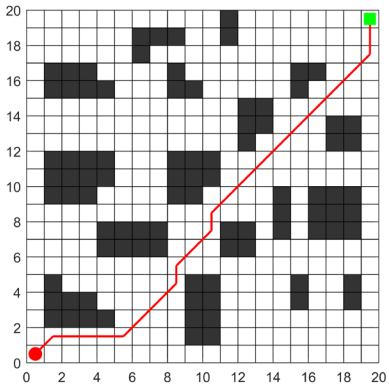

Figure 10. Security marking grid in Scene 1

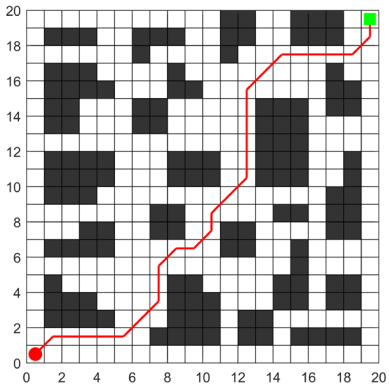

Figure 11. Security marking grid in Scene 2

4.4 Smooth Path-Planning Results

The fusion algorithm using the smoothing method in Scene 1 and Scene 2, respectively, is run. Figures 12 and 13 indicate that the number of corners is 4 and 6, respectively. The optimal path lengths are 28.6540 and 31.3274, respectively. This optimization method utilizes the number of corners as the main indicator for evaluating the quality of the path. This path-planning method can be chosen, if the lowest energy consumption of the transportation robot is a prerequisite.

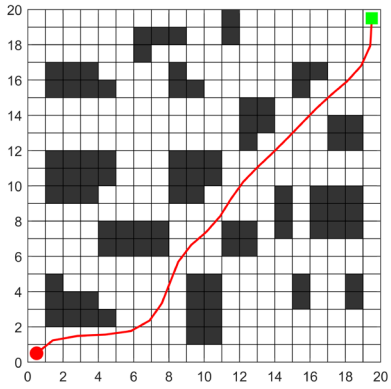

Figure 12. Smooth path in Scene 1

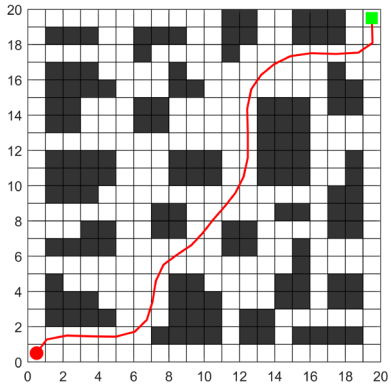

Figure 13. Smooth path in Scene 2

Compared to straight-line movement, any turn generates additional energy consumption, regardless of the specific size of the turning angle. The purpose of this approach is to simplify the calculations, while also preserving the practicality of the model. Given these conditions, the energy consumption formula is defined as follows:

$$E_{sum} = L \cdot E_m + N_t \, E_t \tag{13}$$

where L denotes the total length of the path; N_t, *denote*s the number of turns in the path; E_m denotes the energy consumption for moving one cell forward; and E_t denotes the energy consumption for each turn.

The parameters are as follows: E_m=1, E_t=0.5. The energy consumption values are as follows: 32.7132 (as seen in Figure 10), 38.6421 (as seen in Figure 11), 30.6540 (as seen in Figure 12), and 34.3274 (as seen in Figure 13). Therefore, the smoothed path consumes less energy than the original path.

5. Conclusion

Herein, a path-planning method of a fusion algorithm with complementary advantages is proposed. For the characteristics of material transfer work, three path-planning methods are proposed: the shortest path, the safest path, and the path with the lowest energy consumption. The robot can select the appropriate path according to the characteristics of the material to be transported. By analysing the simulation results, the paths planned by the algorithm are superior to SSA, GA, and PSO. Simultaneously, the sub-strategy-based path planning method proposed herein, tailored to material characteristics, not only enhances the efficiency of shop-floor material transfer robots, but also renders material transportation paths more adaptable. This study provides a basis for researching the application of robot path planning algorithms in planning various types of material transport routes within shop-floor environments.

REFERENCES

Cai, Y., Liu, S. F., Tao, Z. B., Li, C. G., Sun, Y, F. & Ban, J. M. (2018) Path planning of sorting and handling robot based on improved A* algorithm. *Computer Measurement & Control*. 26(4), 164-166. doi: 10.16526/j.cnki.11-4762/tp.2018.04.043.

Chai, G. F. & Xia, Y. Z. (2023) Multi-Robot Path Optimization and Simulation for Multi-Route Inspection in Manufacturing. *The International Journal of Simulation Modelling*. 22(1), 121-132. doi: 10.2507/IJSIMM22-1-CO1.

Chen, Y., Wu, J. F., He, C. S. & Zhang, S. (2023) Intelligent warehouse robot path planning based on improved ant colony algorithm. *IEEE Access*. 11, 12360-12367. doi: 10.1109/ACCESS.2023.3241960.

Chen, Z. H., Wu, H. Y., Chen, Y., Cheng, L. & Zhang, B. Q. (2022) Patrol robot path planning in nuclear power plant using an interval multi-objective particle swarm optimization algorithm. *Applied Soft Computing*. 116, 108192. doi: 10.1016/j.asoc.2021.108192.

Du, L. Z., Ke, S., Wang, Z., Tao, J., Yu, L. Q. & Li, H. J. (2019) Research on multi-load AGV path planning of weaving workshop based on time priority. *Mathematical Biosciences and Engineering: MBE*. 16(4), 2277-2292. doi:10.3934/mbe.2019113.

Gao, W. X., Tang, Q., Ye, B. F., Yang, Y. & Yao, J. (2020) An enhanced heuristic ant colony optimization for mobile robot path planning. *Soft Computing*, 24, 6139-6150. doi: 10.1007/s00500-020-04749-3.

Gong, C., Dai, C. H., Jiang, W., Yu, J. K. & Chen, Z. (2023) Path planning of transport robot in large loom workshop based on improved A* algorithm. *Journal of Advanced Textile Engineering*. 1(5),57-67. doi: 10.3969/j.issn.2095-4131.2023.05.008.

Gu, Y., Duan, J. J., Su, Y. X. & Yuan, Y, Y. (2020) Path planning of warehouse logistics robot based on improved ant colony algorithm. *Journal of Wuhan University of Technology* (*Transportation Science & Engineering*). 44(4), 688-693. doi: 10.3963/j.issn.2095-3844.2020.04.019.

Gültekin, A., Diri, S. & Becerikli, Y. (2023) Simplified and Smoothed Rapidly-Exploring Random Tree Algorithm for Robot Path Planning. *Tehnički vjesnik [Technical Gazette]*. 30(3), 891-898. doi: 10.17559/TV-20221015080721.

Haider, M. H., Wang, Z., Khan, A. A., Ali, H., Zheng, H., Usman, S., Kumar, J., Bhutta, M. U. M. & Zhi, P. (2022) Robust mobile robot navigation in cluttered environments based on hybrid adaptive neuro-fuzzy inference and sensor fusion. *Journal of King Saud University-Computer and Information Sciences*. 34(10), 9060-9070. doi: 10.1016/j.jksuci.2022.08.031.

Hao, M. R. (2022) Design of mine wheeled material transport robot. *Coal Science and Technology*. 50(4), 270-276. doi: 10.13199/j.cnki.cst.2020-0379.

Ibrahim, N., Hassan, F. H., Ab Wahab, M. N. & Letchmunan, S. (2022) Emergency Route Planning with the Shortest Path Methods: Static and Dynamic Obstacles. *The International Journal of Simulation Modelling*. 21(3), 429-440. doi: 10.2507/IJSIMM21-3-608.

Liu, L. X., Wang, X., Yang, X., Liu, H. J., Li, J. P. & Wang, P. F. (2023) Path planning techniques for mobile robots: Review and prospect. *Expert Systems with Applications*. 2023, 120254. doi: 10.1016/j.eswa.2023.120254.

Liu, N., Ma, C. Y., Hu, Z. H., Guo, P. F., Ge, Y. & Tian, M. (2024) Workshop AGV path planning based on improved A* algorithm. *Mathematical Biosciences and Engineering*. 21(2), 2137-2162. doi:10.3934/mbe.2024094.

Mani, V., Yarlagadda, S. R., Ravipati, S., & Swarnamma, S. C. (2023) Ann optimized hybrid

energy management control system for electric vehicles. *Studies in Informatics and Control*. 32(1), 101-110. doi: 10.24846/v32i1y202310.

Pu, X. C, Song, X. L, Tan, L. & Zhang, Y. (2023) Improved ant colony algorithm in path planning of a single robot and multi-robots with multi-objective. *Evolutionary Intelligence*. 17(3), 1313-1326. doi: 10.1007/s12065-023-00821-7.

Saber, A. M., Behiry, M. H. & Amin, M. (2022) Real-time optimization for an AVR system using enhanced Harris Hawk and IIoT. *Studies in Informatics and Control*. 31(2), 81-94. doi: 10.24846/v31i2y202208.

Šegota*, S. B., Anđelić, N., Car, Z. & Šercer, M. (2022) Prediction of Robot Grasp Robustness using Artificial Intelligence Algorithms. *Tehnički vjesnik. [Technical Gazette]*. 29(1), 101-107. doi: 10.17559/TV-20210204092154.

Tao, Q. Y., Sang, H. Y., Guo, H. W. & Wang, P. (2021) Improved particle swarm optimization algorithm for AGV path planning. *IEEE Access*. 9, 33522-33531. doi: 10.1109/ACCESS.2021.3061288.

Tao, X. M., Guo, W. J., Li, X. K., Chen, W. & Wu, Y. K. (2023) Density peak based multi subpopulation particle swarm optimization with dimensionally reset strategy. *Journal of Software*. 34(4), 1850-1869. doi: 10.13328/j.cnki.jos.006432.

Tao, Z. B., Lei, Z. B., Li, C. G., Sun, Y, F. & Zhou, H. B. (2018) Path planning of handling robot based on improved simulated annealing algorithm. *Computer Measurement & Control*. 26(7), 182-185. doi: 10.16526/j.cnki.11-4762/tp.2018.07.040.

Wang, Y. D., Lu, X. C., Song, Y. M., Feng, Y. & Shen, J. R. (2022a) Monte Carlo Tree Search improved Genetic Algorithm for unmanned vehicle routing problem with path flexibility. *Advances in Production Engineering & Management*. 17(4), 425-438. doi: 10.14743/apem2022.4.446

Wang, Y. J., Liu, X. Q., Leng, J. Y., Wang, J. J., Meng, Q. N. & Zhou, M. J. (2022b) Study on scheduling and path planning problems of multi-AGVs based on a heuristic algorithm in intelligent manufacturing workshop. *Advances in Production Engineering & Management*. 17(4), 505-513. doi: 10.14743/apem2022.4.452.

Wen, T., Yang, D. C., Liu, W. F., Wen C. L. & Cai, B. G. (2021) A Novel Integrated Path Planning Algorithm for Warehouse AGVs. *Chinese Journal of Electronics*. 30(2), 331-338. doi:10.1049/cje.2021.02.002.

Wu, L., Huang, X. D., Cui, J. G., Liu, C. & Xiao, W. S. (2023) Modified adaptive ant colony optimization algorithm and its application for solving path planning of mobile robot. *Expert Systems with Applications*. 215, 119410. doi: 1016/j.eswa.2022.119410.

Zhang, M. & Wu, Y. Z. (2023) Optimization of transfer robot path planning based on A* algorithm. *Modern Electronics Technique*. 46(13), 135-139. doi: 10.16652/j.issn.1004-373x.2023.13.023.

Zhang, Y., Li, L. L., Lin, H C., Ma, Z. W. & Zhao, J. (2019) Development of path planning approach using improved a-star algorithm in AGV system. *Journal of Internet Technology*. 20, 915-924. doi: 10.3966/160792642019052003023.

Zhong, X. Y., Tian, J., Hu, H. & Peng, X. F. (2020) Hybrid path planning based on safe A* algorithm and adaptive window approach for mobile robot in large-scale dynamic environment. *Journal of Intelligent & Robotic Systems*. 99(1), 65-77. doi: 10.1007/s10846-019-01112-z.

Zhou, H. W., Sun, L. P., Dai, L. X. & Guo, T. T. (2014) Wood processing workshop floor cleaning robot dynamic obstacle avoidance path planning research. *Journal of Northeast Forestry University*. 42(6), 143-147. doi: 10.13759/j.cnki.dlxb.20140523.002.

Zhou, J. (2020) Workshop used robot navigation path planning method based on chaotic wolf pack besieging algorithm. *Machinery Design & Manufacture*. 2020(1), 251-255. doi: 10.3969/j.issn.1001-3997.2020.01.062.

Zhu, Y., Li, Y. P., Zhang, Y. W. & Li, W. J. (2020) Handling robot path planning based on improved artificial potential field method. *Electronic Measurement Technology*. 43(17), 101-104. doi: 10.19651/j.cnki.emt.2004627.